Control and analysis of a unified power flow controller

Hideaki Fujita
Okayama University

Yasuhiro Watanabe
Okayama University

Hirofumi Akagi
Okayama University

Control and Analysis of a Unified Power Flow Controller

Hideaki Fujita, *Member, IEEE,* Yasuhiro Watanabe, and Hirofumi Akagi, *Fellow, IEEE*

***Abstract*— This paper presents a control scheme and comprehensive analysis for a unified power flow controller (UPFC) on the basis of theory, computer simulation, and experiment. This developed theoretical analysis reveals that a conventional power-feedback control scheme makes the UPFC induce power fluctuation in transient states. The conventional control scheme cannot attenuate the power fluctuation, and so the time constant of damping is independent of active- and reactive-power feedback gains integrated in its control circuit. This paper proposes an advanced control scheme which has the function of successfully damping out the power fluctuation. A UPFC rated at 10 kVA is designed and constructed, which is a combination of a series device consisting of three single-phase pulsewidth modulation (PWM) converters and a shunt device consisting of a three-phase diode rectifier. Although the dynamics of the shunt device are not included, it is possible to confirm and demonstrate the performance of the series device. Experimental results agree well with both analytical and simulated results and show viability and effectiveness of the proposed control scheme.**

***Index Terms*— High-power PWM converters, power feedback control, power fluctuation, unified power flow controllers.**

I. Introduction

In RECENT years, environmental, right-of-way, and cost concerns have delayed the construction of both power stations and new transmission lines, while the demand for electronic energy has continued to grow in many countries. This situation has spurred interest in providing already-existing power systems with greater operating flexibility and better utilization. The flexible ac transmission systems (FACTS) concept [1], based on applying leading-edge power electronics technology to existing ac transmission systems, improves stability to increase usable power transmission capacity to its thermal limit. A unified power flow controller (UPFC) [1]–[7], which is one of the most promising devices in the FACTS concept, has the potential of power flow control and/or voltage stability in power transmission systems.

Little literature has been published on theoretical analysis in transient states, although not only feasibility studies, but also practical implementations of the UPFC are presently under way. Undeland *et al.* have proposed a control scheme for the UPFC, with the focus on dynamic as well as static performance [4]. This control scheme, referred to as "cross-coupling control," adjusts the q-axis voltage v_q to control the d-axis current i_d and the d-axis voltage v_d to control the q-axis current i_q. Computer simulation and experimental results with emphasis on dynamic performance have been shown in [4], but theoretical analysis would not be enough to support the experimental results.

This paper deals with control and analysis for a UPFC on the basis of theory, computer simulation, and experiment. Theoretical analysis in transient states is performed with focus on "power fluctuations" which are somewhat similar to "power swings" understood by power system engineers. However, the power fluctuations discussed in this paper are high-frequency (more than 100 Hz) oscillations associated with control of the UPFC, whereas the power swings are low-frequency (less than 1 Hz) oscillations related to the moments of inertia of turbine alternators. Thus, the power fluctuations may occur even when the phase angles of the sending and receiving ends are fixed. This paper theoretically derives that a conventional power-feedback control scheme makes the UPFC induce power fluctuation in transient states, and that the time constant of damping is independent of active- and reactive-power feedback gains integrated in its control circuit. This paper proposes an advanced control scheme intended for successfully damping the power fluctuation in transient states. This control scheme makes the UPFC act as a "damping resistor" against the power fluctuation. This stems from the concept that the series active filter proposed in [8] has the function of harmonic damping.

Experimental results obtained from a UPFC rated at 10 kVA are shown to verify the theoretical analysis and viability of the proposed control system. As the first of a step-by-step approach, a three-phase diode rectifier is used as a shunt device in the experiment, so that the dynamics of the shunt device are not included in the experimental results. However, the "interim" results obtained from the 10-kVA UPFC agree with both analytical and simulated results and show that the advanced control scheme is viable and effective both in damping out the power fluctuation and in eliminating steady-state errors.

II. Basic Configuration of a UPFC

Fig. 1 shows a system configuration of a general UPFC, which is installed between the sending end V_S and the receiving end V_R. The UPFC consists of a combination of a series device and a shunt device, the dc terminals of which are connected to a common dc-link capacitor. The series device acts as a controllable voltage source V_C, whereas the shunt device acts as a controllable current source I_C. The main purpose of the shunt device is to regulate the dc-

Manuscript received July 6, 1998; revised April 20, 1999. Recommended by Associate Editor, F. Peng.

The authors are with the Department of Electrical Engineering, Okayama University, Okayama 700-8530, Japan.

Publisher Item Identifier S 0885-8993(99)08900-0.

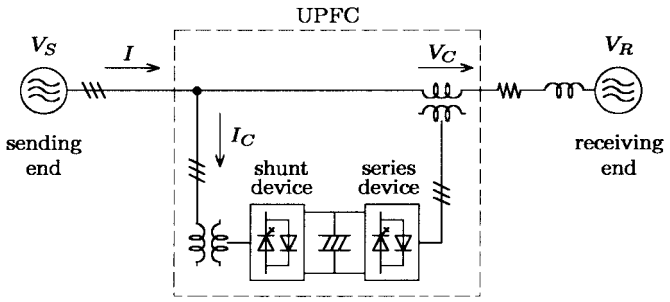

Fig. 1. System configuration of a general UPFC.

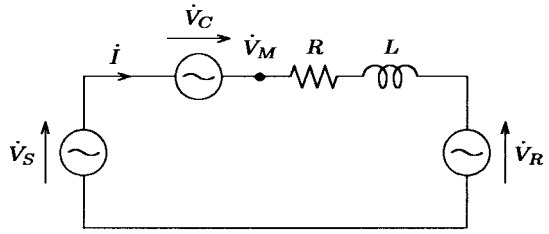

Fig. 2. Single-phase equivalent circuit.

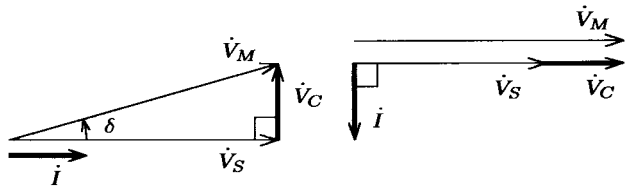

Fig. 3. Phasor diagrams in case of active and reactive power control: (a) active power control and (b) reactive power control.

link voltage by adjusting the amount of active power drawn from the transmission line. In addition, the shunt device has the capability of controlling reactive power. In the following discussion, the shunt device is disregarded because the current flowing into the shunt device, I_C is not as large as the transmission line current I.

Fig. 2 shows a single-phase equivalent circuit of the UPFC, where the reactor L and the resistor R represent inductance and resistance in the transmission line, respectively. It is reasonable to remove the line resistance R because $\omega_0 L \gg R$ in the overhead transmission line. Thus, the line current phasor vector $\dot{I}$ is given by

$$\dot{I} = \frac{\dot{V}_S - \dot{V}_R + \dot{V}_C}{j\omega_0 L}. \tag{1}$$

For the sake of simplicity, the assumption of $\dot{V}_S = \dot{V}_R$ leads to the phasor diagrams shown in Fig. 3. When the output voltage $\dot{V}_C$ leads by 90° with respect to $\dot{V}_S$, $\dot{I}$ is in phase with $\dot{V}_S$, as shown in Fig. 3(a). This results in achieving active-power flow from $\dot{V}_S$ to $\dot{V}_R$. Controlling $\dot{V}_C$ to be in phase with $\dot{V}_S$ makes $\dot{I}$ lag by 90° with respect to $\dot{V}_S$, thus resulting in reactive-power flow, as shown in Fig. 3(b). Since the phasor vectors are applied, the above discussion is not applicable to analysis of the dynamic behavior.

III. Conventional Control Schemes

A. Phase-Angle Control

Adjusting the amplitude of the 90° leading or lagging output voltage makes it possible to control active power. On the d-q frame coordinates based on space vectors, the d-axis current i_d corresponds to active power, and so it can be controlled by the q-axis voltage v_{Cq}. Therefore, the voltage reference vector $\boldsymbol{v}_{\boldsymbol{C}}^{*} = [v_{Cd}^{*}, v_{Cq}^{*}]^t$ for the series device is given by

$$\begin{bmatrix} v_{Cd}^{*} \\ v_{Cq}^{*} \end{bmatrix} = \begin{bmatrix} 0 & 0 \\ K_p & 0 \end{bmatrix} \begin{bmatrix} i_d^{*} - i_d \\ i_q^{*} - i_q \end{bmatrix} \tag{2}$$

where K_p [V/A] is an active-power feedback gain and i_d^{*} and i_q^{*} are active- and reactive-current references, respectively. Then the phase angle between $\dot{V}_M$ and $\dot{V}_S$ (δ) can be controlled by V_{Cq} as follows:

$$\delta = \tan^{-1}\left(\frac{V_{Cq}}{V_S}\right).$$

Thus, this control scheme is identical with the so-called "phase-angle control" which is one of the most basic control schemes for the UPFC.

B. Cross-Coupling Control

The "cross-coupling control" proposed in [4] has not only an active-power feedback loop, but also a reactive-power feedback loop. This control scheme is characterized by controlling both the magnitude of $\dot{V}_M$ and the phase angle δ. As a result, the cross-coupling control enables the UPFC to achieve both active- and reactive-power control. On the d-q frame coordinates, the q-axis current i_q corresponds to reactive power and so it can be controlled by v_{Cd}. Therefore, the voltage reference for the series device is given by

$$\begin{bmatrix} v_{Cd}^{*} \\ v_{Cq}^{*} \end{bmatrix} = \begin{bmatrix} 0 & -K_q \\ K_p & 0 \end{bmatrix} \begin{bmatrix} i_d^{*} - i_d \\ i_q^{*} - i_q \end{bmatrix} \tag{3}$$

where K_q [V/A] is a feedback gain of reactive power.

The phase-angle and cross-coupling control schemes seem to be on the basis of space vectors. However, neither control schemes may render good dynamic performance because interference exists in voltage and current between the d axis and the q axis. The series device injects a q-axis voltage to control the d-axis current or the active power in both control schemes. The q-axis voltage, however, induces the q-axis current to flow in a transient state. Therefore, the active-power flow control is accompanied by the reactive-power flow control even though either control scheme provides instantaneous voltage references.

IV. Advanced Control Scheme and Transient Analysis

A. Advanced Control Scheme

This paper proposes an advanced control scheme. The reference voltage vector for the series device $\boldsymbol{v}_{\boldsymbol{C}}^{*}$ is generalized as follows:

$$\begin{bmatrix} v_{Cd}^{*} \\ v_{Cq}^{*} \end{bmatrix} = \begin{bmatrix} K_r & -K_q \\ K_p & K_r \end{bmatrix} \begin{bmatrix} i_d^{*} - i_d \\ i_q^{*} - i_q \end{bmatrix}. \tag{4}$$

Note that the control scheme comprehends both phase angle and cross-coupling control schemes, so that it can be considered a generalized control scheme for the UPFC. This scheme has two additional terms with identical gain K_r. A voltage vector produced by the two terms is in phase with a current error vector of $\boldsymbol{i^* - i}$. This means that the UPFC acts as a damping resistor against a current error of $\boldsymbol{i - i^*}$, paying attention to the polarity of $\boldsymbol{v_C}$ in Fig. 2.

B. Transient Analysis

The following assumptions are made in transient analysis.

1) The sending-end voltage v_S is equal to the receiving-end voltage v_R, and they are three-phase balanced sinusoidal voltage sources.
2) The series device is assumed to be an ideal controllable voltage source. Therefore, the output voltage vector $\boldsymbol{v_C}$ is equal to its reference $\boldsymbol{v_C^*}$.

Invoking the first assumption yields $\mathbf{v}_S$ as follows:

$$\begin{bmatrix} v_{Su} \\ v_{Sv} \\ v_{Sw} \end{bmatrix} = \sqrt{\frac{2}{3}} V_S \begin{bmatrix} \cos\omega_0 t \\ \cos(\omega_0 t - 2\pi/3) \\ \cos(\omega_0 t + 2\pi/3) \end{bmatrix} \tag{5}$$

where V_S is an rms voltage at the sending end, and ω_0 is a supply angular frequency. The equivalent circuit shown in Fig. 2 provides the following:

$$\left(R + L\frac{d}{dt}\right) \begin{bmatrix} i_u \\ i_v \\ i_w \end{bmatrix} = \begin{bmatrix} v_{Cu} \\ v_{Cv} \\ v_{Cw} \end{bmatrix}. \tag{6}$$

Applying the d-q transformation to (5) and (6) leads to

$$\begin{bmatrix} v_{Sd} \\ v_{Sq} \end{bmatrix} = \begin{bmatrix} V_S \\ 0 \end{bmatrix} \tag{7}$$

$$\begin{bmatrix} R + L\frac{d}{dt} & -\omega_0 L \\ \omega_0 L & R + L\frac{d}{dt} \end{bmatrix} \begin{bmatrix} i_d \\ i_q \end{bmatrix} = \begin{bmatrix} v_{Cd} \\ v_{Cq} \end{bmatrix}. \tag{8}$$

The instantaneous active and reactive powers [9] p and q are given by

$$\begin{bmatrix} p \\ q \end{bmatrix} = \begin{bmatrix} v_{Sd} \cdot i_d + v_{Sq} \cdot i_q \\ v_{Sd} \cdot i_q - v_{Sq} \cdot i_d \end{bmatrix} = V_S \begin{bmatrix} i_d \\ i_q \end{bmatrix}. \tag{9}$$

Substituting (4) into (8), along with invoking the second assumption, gives the following:

$$\begin{bmatrix} R + K_r + L\frac{d}{dt} & -(\omega_0 L + K_q) \\ \omega_0 L + K_p & R + K_r + L\frac{d}{dt} \end{bmatrix} \begin{bmatrix} i_d \\ i_q \end{bmatrix} = \begin{bmatrix} K_r i_d^* - K_q i_q^* \\ K_p i_d^* + K_r i_q^* \end{bmatrix}. \tag{10}$$

Under the assumption of $i_d(0) = i_q(0) = 0$, the Laplace functions for the active and reactive powers produce $I_d(s)$ and $I_q(s)$ as follows:

$$I_d(s) = \frac{(K_r L s + A_1) I_d^* - (K_q L s + A_2) I_q^*}{L^2\left(s^2 + \frac{2(K_r + R)}{L} s + \omega_n^2\right)} \tag{11}$$

$$I_q(s) = \frac{(K_p L s + A_3) I_d^* + (K_r L s + A_4) I_q^*}{L^2\left(s^2 + \frac{2(K_r + R)}{L} s + \omega_n^2\right)} \tag{12}$$

where

$$\begin{aligned} A_1 &= K_p(\omega_0 L + K_q) + K_r(R + K_r) \\ A_2 &= K_q R - K_r \omega_0 L \\ A_3 &= K_p R - K_r \omega_0 L \\ A_4 &= K_q(\omega_0 L + K_p) + K_r(R + K_r) \\ \omega_n &= \frac{\sqrt{(\omega_0 L + K_p)(\omega_0 L + K_q) + (K_r + R)^2}}{L}. \end{aligned}$$

Here, ω_n is an undamped natural frequency. Equations (11) and (12) conclude that the UPFC exhibits a second-order system, thus causing power fluctuation in transient states. Damping factor ζ and fluctuating frequency ω are given as follows:

$$\zeta = \frac{K_r + R}{\sqrt{(\omega_0 L + K_p)(\omega_0 L + K_q) + (K_r + R)^2}} \tag{13}$$

$$\begin{aligned} \omega &= \omega_n \sqrt{1 - \zeta^2} \\ &= \frac{\sqrt{(\omega_0 L + K_p)(\omega_0 L + K_q)}}{L}. \end{aligned} \tag{14}$$

Equation (13) tells us that the larger the gain K_r, the closer ζ is to unity. Equation (14) leads to the fact that the larger the power feedback gains K_p and K_q, the larger the fluctuating frequency ω. The time constant of damping of power fluctuation, τ is given by

$$\tau = \frac{1}{\zeta \omega_n} = \frac{L}{K_r + R}. \tag{15}$$

Note that K_r acts as a damping resistor. Therefore, increasing K_r reduces the time constant and improves the transient stability. The phase-angle control and cross-coupling control schemes have no capability of damping power fluctuation because $K_r = 0$.

Equations (13)–(15) are applicable only to a proportional controller (P controller) without any integral gains. In a real system, a proportional and integral controller (PI controller) should be used to eliminate steady-state errors in active and reactive power. The transfer function of a UPFC with the PI controller is no longer a second-order system. However, the gain K_r acts as a damping resistor for the power fluctuation, irrespective of either the P controller or the PI controller. This leads to significant improvement of dynamic performance of the series device.

V. Experimental System Configuration

A. Main Circuit

Fig. 4 and Table I show a main circuit of an experimental system rated at 10 kVA and its circuit parameters. The main circuit of the series device consists of three single-phase H-bridge voltage-fed pulsewidth modulation (PWM) inverters. A PWM control circuit compares reference voltage $\boldsymbol{v_C^*}$ with a triangle carrier signal of $f_{\mathrm{SW}} = 1$ kHz in order to generate twelve gate signals. An equivalent switching frequency is 2 kHz, which is twice as high as f_{SW} because three H-bridge PWM inverters are used. The ac terminals of the PWM inverters are connected in series through matching transformers with a turn ratio of 1:12. Since the rms voltage of the series device is 12 V, a kilovoltampere rating of the

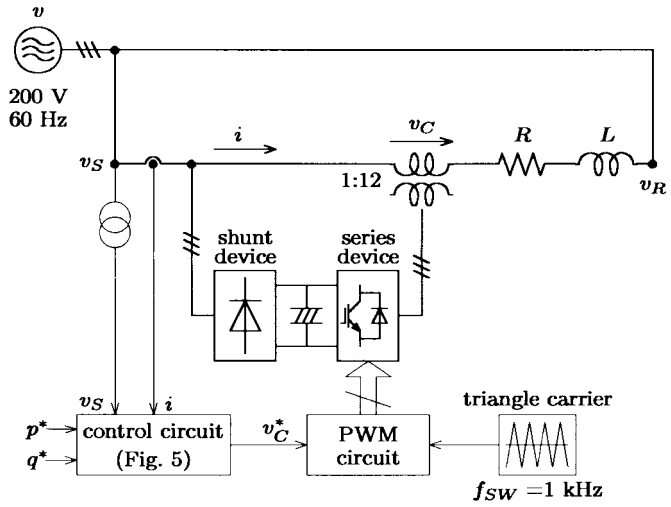

Fig. 4. Main circuit of an experimental system.

TABLE I
EXPERIMENTAL SYSTEM PARAMETERS

Controllable power rating	P	10 kW
Series device capacity	P_{INV}	1.1 kVA (=11%)
Rms voltage of v_C	V_C	±12 V (=10%)
Utility line-to-line voltage	V	200 V
Utility angular frequency	ω_0	$2\pi \times 60$ rad/s
Line inductance	L	1.0 mH (=10%)
Line resistance	R	0.04 Ω (=1%)

3ϕ, 200-V, 10-kVA, 60-Hz base

series device is given by

$$3 \times 12^{\mathrm{V}} \times 30^{\mathrm{A}} = 1.1 \text{ kVA}$$

which is 11% of the controllable active power of 10 kW flowing between v_S and v_R.

A three-phase diode rectifier is employed as the shunt device. A reactor L and a resistor R, representing the impedance of the transmission line, are inserted between v_S and v_R. The sending and receiving ends of the transmission line v_S and v_R are connected to a common power supply v. Thus, no power flow occurs as long as the series device is not operated. Once the series is operated, it always delivers a small amount of active power to the transmission line, which equals the power loss dissipated in the resistor R. A three-phase PWM rectifier should be employed as the shunt device in a practical system because the magnitude and phase of v_S may differ from those of v_R. While the series device draws active power from the transmission line, the shunt device should regenerate the active power from the dc-link capacitor to the transmission line.

B. Control Circuit

Fig. 5 shows a block diagram of the control circuit. The three- to two-phase transformation obtains i_α and i_β from the three-phase currents i_u, i_v, and i_w. The d-q transformation yields i_d and i_q from i_α and i_β with the help of sinusoidal signals of $\sin\omega_0 t$ and $\cos\omega_0 t$ taken from a read-only memory

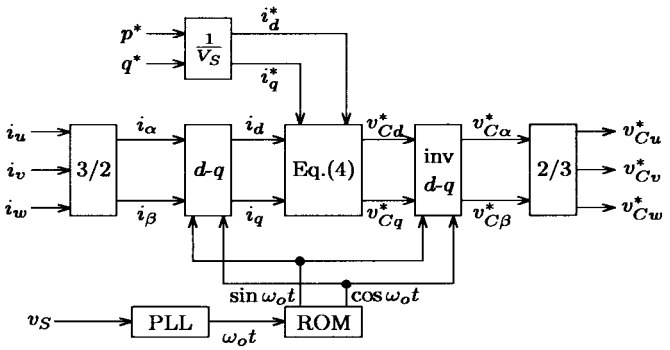

Fig. 5. Control circuit.

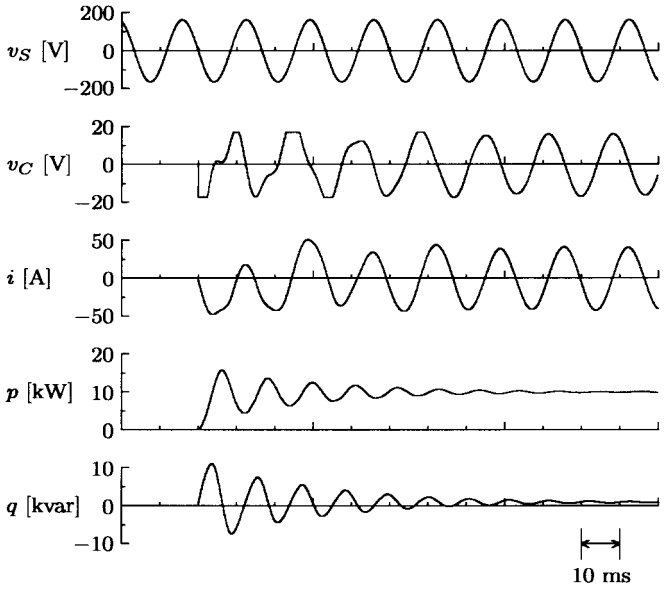

(a)

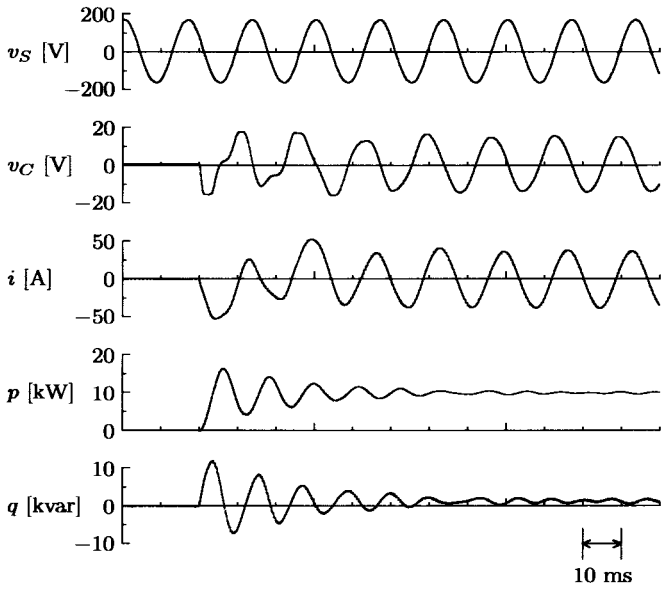

(b)

Fig. 6. Simulated and experimental waveforms when the phase-angle control scheme is applied, $K_p = 0.5$ V/A, and $p^* = 16.5$ kW: (a) simulated waveforms and (b) experimental waveforms.

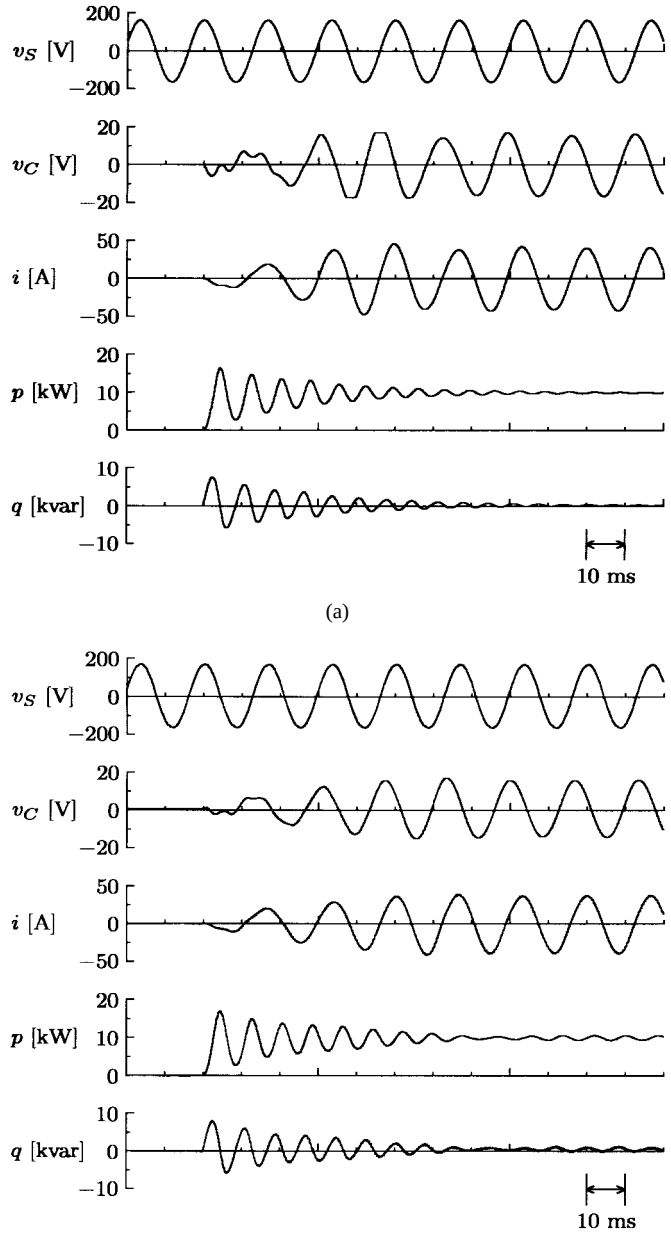

Fig. 7. Simulated and experimental waveforms when the cross-coupling control scheme is applied, $K_p = K_q = 0.5$ V/A, and $p^* = 16.5$ kW, $q^* = 0$: (a) simulated waveforms and (b) experimental waveforms.

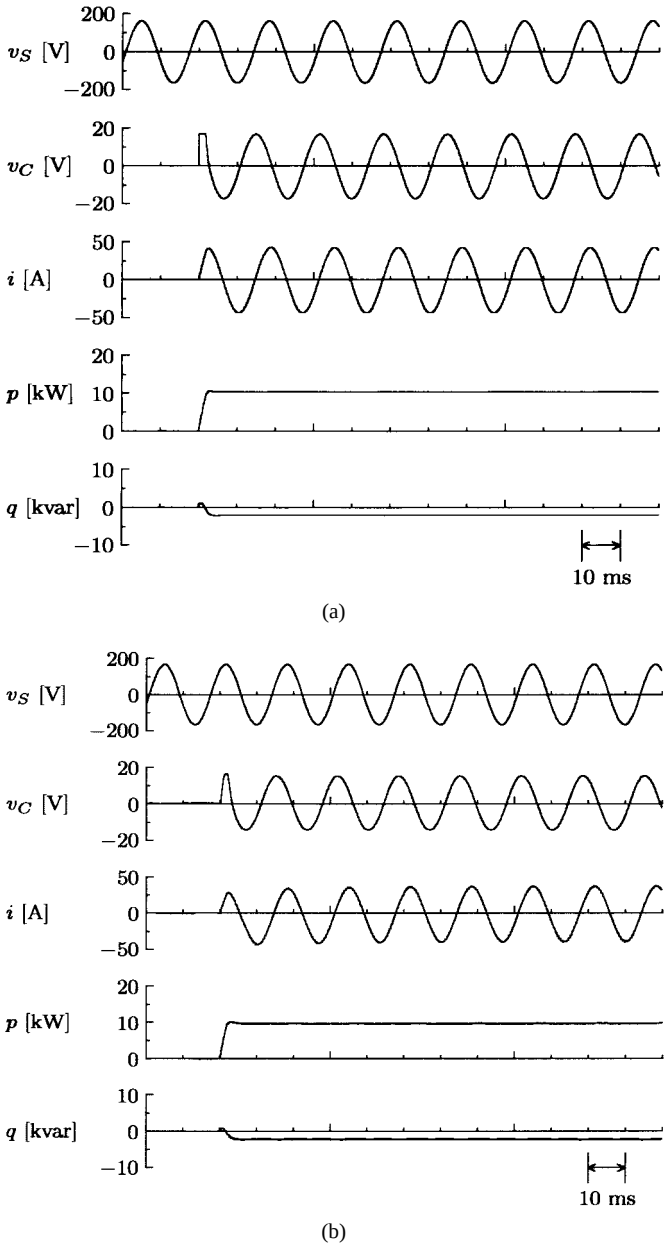

Fig. 8. Simulated and experimental waveforms when the proposed control scheme with P gain is applied, $K_p = K_q = 0.5$ V/A, $K_r = 1.2$ V/A, $p^* = 12$ kW, and $q^* = 0$: (a) simulated waveforms and (b) experimental waveforms.

(ROM). The phase information $\omega_0 t$ is generated by a phase-lock-loop (PLL) circuit. Then v_{Cd}^* and v_{Cq}^* are given by (4).

The power feedback gains are set to $K_p = K_q = 0.5$ V/A in the following experiments. From (13), the feedback gain K_r is obtained as

$$K_r = \frac{\zeta\sqrt{(\omega_0 L + K_p)(\omega_0 L + K_q)}}{\sqrt{1-\zeta^2}} - R. \tag{16}$$

In order to get a damping factor of $\zeta = 0.8$, K_r should be designed as

$$K_r = \frac{0.8\sqrt{(2\pi \times 60 \times 0.001 + 0.5)^2}}{\sqrt{1-0.8^2}} - 0.04 = 1.13 \text{ V/A}.$$

The gain K_r is set to 1.2 V/A in the following experiment.

VI. Simulated and Experimental Results

Figs. 6–9 show simulated and experimental waveforms for a step change in the active power reference p^*. Tables II and III show experimental and theoretical values of damping factor ζ, fluctuating frequency ω, and damping time constant τ. The experimental waveforms of the series device voltage v_C are measured through a low-pass filter with a cutoff frequency of 400 Hz because the switching frequency of the series device is 1 kHz. Circuit simulation software based on PSpice is used to calculate the simulated results, and then the series device is assumed to be an ideal controllable voltage source which is equal to the voltage reference v_C^*. Note that step references for the three control schemes are set to different values in order to

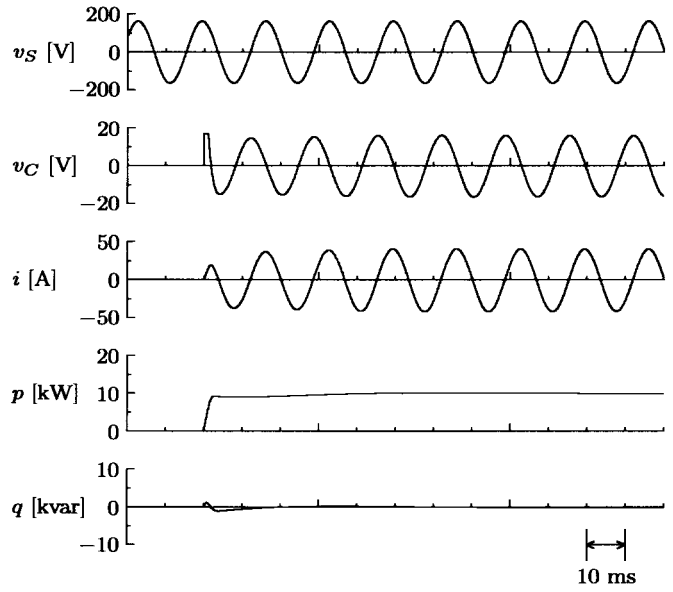

(a)

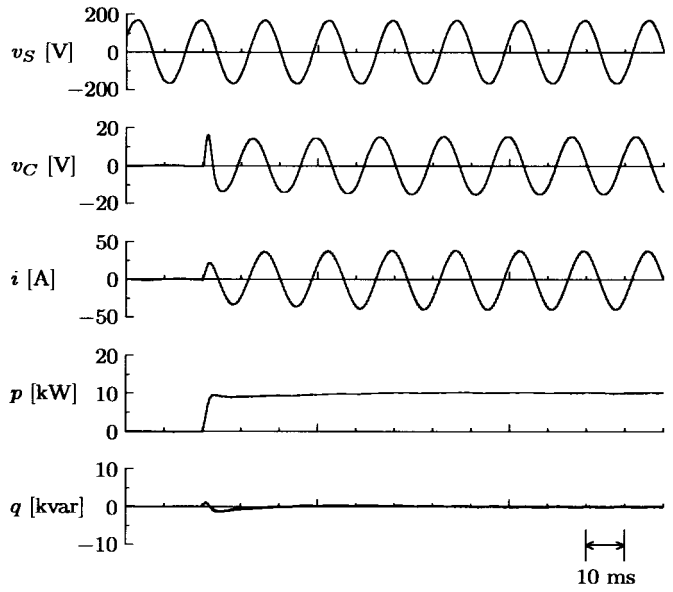

(b)

Fig. 9. Simulated and experimental waveforms when the proposed control scheme with PI gain is applied, $K_p = K_q = 0.5$ V/A, $K_r = 1.2$ V/A, $T_I = 5$ ms, $p^* = 10$ kW, and $q^* = 0$: (a) simulated waveforms and (b) experimental waveforms.

adjust their final values to 10 kW and compare only damping performance.

Fig. 6 shows waveforms when the phase-angle control scheme is applied. The simulated and experimental waveforms agree well with each other, not only in the steady state, but also in the transient state. Nonnegligible power fluctuation with a frequency of 520 rad/s occurs in the waveforms of p and q. After the step change, p and q reach their final values in 70 ms. Equation (15) determines the theoretical time constant

$$\tau = \frac{L}{K_r + R} = \frac{1.0 \text{ mH}}{0 + 0.04\ \Omega} = 25 \text{ ms}$$

which agrees well with the experimental value in Table II. Decreasing the control gain K_p may enable suppression of the power fluctuation, but it is accompanied by increasing steady-state error in p.

TABLE II
EXPERIMENTAL AND THEORETICAL VALUES OF DAMPING FACTOR ζ, FLUCTUATING FREQUENCY ω, AND DAMPING TIME CONSTANT τ

Control Schemes	ζ	ω [rad/s]	τ [ms]
phase-angle control (Fig. 6)	0.067	520	28
cross-coupling control (Fig. 7)	0.053	740	26
proposed control (Fig. 8)	0.76	900	0.95

TABLE III
THEORETICAL VALUES OF DAMPING FACTOR ζ, FLUCTUATING FREQUENCY ω, AND DAMPING TIME CONSTANT τ

Control Schemes	ζ	ω [rad/s]	τ [ms]
phase-angle control (Fig. 6)	0.069	570	25
cross-coupling control (Fig. 7)	0.046	880	25
proposed control (Fig. 8)	0.82	880	0.81

Fig. 7 shows waveforms when the cross-coupling control scheme is applied. It is clear from (14) that addition of the reactive power feedback gain K_q increases the fluctuating frequency ω from 520 to 740 rad/s. Since (15) shows that the time constant τ is independent of K_p and K_q, it takes 70 ms to reach their steady-state values.

Fig. 8 shows waveforms when the advanced control scheme proposed in this paper is applied. No power fluctuation occurs in p and q. From (15), the theoretical time constant is

$$\tau = \frac{L}{K_r + R} = \frac{1.0 \text{ mH}}{1.2 + 0.04\ \Omega} = 0.81 \text{ ms}$$

which is superior to those of both conventional control schemes. The proposed control scheme has the capability of damping power fluctuation and improving transient characteristics. Then the step reference p^* is 12 kW, which is smaller than that in Figs. 6 and 7. This means that the advanced control can reduce the steady-state error in p. However, steady-state error in q appears in Fig. 8, while it is almost zero in Figs. 6 and 7.

Fig. 9 shows waveforms under the same conditions as Fig. 8 except for adding integral gains to K_p and K_q. The integral gain is set so as to be $T_I = 5$ ms, so that the steady-state errors are removed from p and q. Note that addition of the integral gain has no effect on damping of power fluctuation although the UPFC is no longer a second-order system.

VII. CONCLUSION

This paper has proposed an advanced control scheme for a UPFC, along with a comprehensive analysis. The experimental results obtained from a UPFC rated at 10 kVA has shown concurrence with analytical results. The experimental setup is not a full UPFC because a three-phase diode rectifier is used as the shunt device. Thus, the dynamics of the shunt device are not included in the experimental results. The "interim" results, however, have resulted in the following essentials related to the control and performance of the series device.

- A conventional feedback control of power flow makes the UPFC induce power fluctuation in transient states.
- The time constant of damping out the fluctuation is independent of feedback gains for active and reactive power. Therefore, the conventional control schemes based on power feedback loops has little capability to damp out the power fluctuation.
- The advanced control scheme proposed in this paper achieves a quick response of active and reactive power without either causing power fluctuation or producing steady-state errors.

REFERENCES

[1] L. Gyugyi, "Unified power-flow control concept for flexible ac transmission systems," *Proc. Inst. Elect. Eng.*, vol. 139, pt. C, pp. 323–331, July 1992.
[2] B. T. Ooi, S. Z. Dai, and X. Wang, "Solid-state series capacitive reactance compensators," *IEEE Trans. Power Delivery*, vol. 7, no. 2, pp. 914–919, 1990.
[3] B. S. Rigby and R. G. Harley, "An improved control scheme for a series capacitive reactance compensator based on a voltage source inverter," in *IEEE/IAS Annu. Meeting*, 1996, pp. 870–877.
[4] Q. Yu, S. D. Round, L. E. Norum, and T. M. Undeland, "Dynamic control of a unified power flow controller," in *IEEE PESC'96*, pp. 508–514.
[5] L. Gyugyi, C. D. Schauder, and K. K. Sen, "Static synchronous series compensator: A solid-state approach to the series compensation of transmission lines," *IEEE Trans. Power Delivery*, vol. 12, no. 1, pp. 406–413, 1997.
[6] Y. Jiang and A. Ekstrom, "Optimal controller for the combination system of a UPFC and conventional series capacitors," in *EPE'97*, vol. 1, pp. 372–337.
[7] Y. Chen, B. Mwinyiwiwa, Z. Wolanski, and B. T. Ooi, "Unified power flow controller (UPFC) based on chopper stabilized multilevel converter," in *IEEE PESC'97*, pp. 331–337.
[8] F. Z. Peng, H. Akagi, and A. Nabae, "A new approach to harmonic compensation in power systems—A combined system of shunt passive and series active filters," *IEEE Trans. Ind. Applicat.*, vol. 26, no. 6, pp. 983–990, 1990.
[9] H. Akagi, Y. Kanazawa, and A. Nabae, "Instantaneous reactive power compensators comprising switching devices without energy storage components," *IEEE Trans. Ind. Applicat.*, vol. 20, no. 3, pp. 625–630, 1984.

Hideaki Fujita (M'91), for a photograph and biography, see this issue, p. 1020.

Yasuhiro Watanabe was born in Gifu, Japan, on May 16, 1972. He received the B.S. degree in electrical engineering from Shizuoka University in 1995 and the M.S. degree from Okayama University, Okayama, Japan, in 1997. He is currently working towards the Ph.D. degree in power electronics at Okayama University.

Hirofumi Akagi (M'87–SM'94–F'96), for a photograph and biography, see this issue, p. 1020.